Tissue and Cell 104 (2027) 104039

Contents lists available at ScienceDirect

Tissue and Cell

journal homepage: www.elsevier.com/locate/tice

Curcumin loaded solid lipid nanoparticles ameliorates poly (I:C)-induced exacerbation of allergic asthma

Ayushi Sandhu [a], Divya [b], Nidhi Verma [a], Indu Pal Kaur [b], Amarjit S. Naura [a,*]

[a] Department of Biochemistry, Panjab University, Chandigarh, 160014, India
[b] University Institute of Pharmaceutical Sciences, Panjab University, Chandigarh, 160014, India

ARTICLE INFO

Keywords:
Asthma exacerbation
Viral infection
Curcumin-loaded solid lipid nanoparticles
Inflammation
Oxidative stress

ABSTRACT

Virus-mediated asthma exacerbations represent a major clinical burden, characterized by neutrophilic inflammation, airway hyperresponsiveness, and oxidative stress leading to the worsening of asthma symptoms. Recently, we have reported that poly (I:C)-mediated asthma exacerbation is unresponsive to dexamethasone (corticosteroid class of drugs) underscoring the need for alternative therapeutic strategy. Given the well-established anti-inflammatory and antioxidant potential of curcumin, the present study aimed at investigating the protective potential of curcumin loaded solid lipid nanoparticles (SLNs) against poly (I:C) mediated exacerbation of allergic asthma in mice and SLN preparation and characterization. OVA + poly (I:C) exposed mice were orally administered curcumin loaded SLNs prior to each poly (I:C) instillation for three consecutive days. Twenty four hours after last poly (I:C) challenge, BALF/lung tissues were procured for the analysis of inflammatory cells and molecular players. Pretreatment of OVA + poly (I:C) exposed mice with curcumin-loaded SLNs ameliorated the robust influx of inflammatory cells along with reduction in the expression of inflammatory mediators including TNF-α, IL-6, G-CSF, and KC in the lungs of mice. This was accompanied by normalization of airway hyperresponsiveness and mucus hypersecretion. Protection exerted by curcumin-loaded SLNs was linked with blunted activation of p38MAPK. Further, our nano formulation improved the redox balance potentially through enhanced expression of Nrf2. Overall, our data shows that curcumin-loaded SLNs protects against poly (I:C)-mediated inflammation in allergic asthma by modulating inflammatory and oxidative pathways and thus may serve as a promising preventive/therapeutic candidate for managing virus mediated asthma exacerbations.

1. Introduction

Asthma is a chronic inflammatory airway disease characterized by episodic airflow obstruction and airway hyperresponsiveness. A small proportion of individuals suffer from sudden, acute episodes of worsening of asthma symptoms often associated with progressive decline in lung functions which frequently lead to increased disease-related morbidity and cause a greater burden on healthcare resources often classified as 'exacerbations' (Park and Tantisira, 2017; Kim et al., 2018). Respiratory viral infections, predominantly rhinoviruses and respiratory syncytial virus, are identified in nearly 80% of exacerbation patients underscoring viral susceptibility as critical determinant of disease severity (Feddema and Claassen, 2020). These respiratory viruses use single-stranded RNA (ssRNA) to encode their genome with double-stranded RNA (dsRNA) as an intermediate during viral replication, which can be sensed by the toll-like receptor (TLR) 3 present on various immune cells including macrophages, neutrophils, and non-immune cells like airway smooth muscle cells, and epithelial and endothelial cells (Lunding et al., 2015). Poly (I:C), a well-established viral surrogate is often used to mimic viral infections in both *in vitro* and *in vivo* studies. Recently, we have reported that poly (I:C) treatment in OVA-sensitized and challenged mice effectively mimics the key features of viral mediated exacerbation of allergic asthma which respond poorly to dexamethasone, a corticosteroid class of drugs. Therefore, alternative preventive/therapeutic strategies are urgently needed to combat the exacerbated symptoms associated with asthma exacerbations triggered by seasonal viral infections in susceptible individuals.

The perennial herb Curcuma longa, commonly known as turmeric, belonging to Zingerberaceae family, is widely cultivated in tropic and subtropics of Asia, especially in India, China, and Indonesia. Curcumin

* Corresponding author.
E-mail addresses: ayushisandhu11@gmail.com (A. Sandhu), divyaapandit09@gmail.com (Divya), nidhiverma.pu@gmail.com (N. Verma), indupalkaur@pu.ac.in (I.P. Kaur), anaura@pu.ac.in (A.S. Naura).

https://doi.org/10.1016/j.tice.2026.104039
Received 9 June 2026; Received in revised form 30 September 2026; Accepted 6 October 2026
Available online 8 October 2026
0040-8166/© 2026 Elsevier Ltd. All rights are reserved, including those for text and data mining, AI training, and similar technologies.

(1,7 bis(4-hydroxy-3-methoxyphenyl)-1,6-heptadiene-3,5-dione), a yellow polyphenol, is one of the main bioactive molecules isolated from turmeric (Abd El-Hack et al., 2021). Curcumin exhibits broad-spectrum of biological activities including anti-tumour, anti-bacterial, anti-oxidant, and anti-inflammatory properties which has led to its extensive use for treatment of several diseases (Tang et al., 2021; Fan et al., 2015; Peng KT et al., 2019). Due to low bioavailability, and poor aqueous solubility of curcumin, its clinical utility remains limited. To overcome these problems, drug delivery systems like polymer, chitosan, and solid lipid nanoparticles were employed for better bioavailability and targeted delivery of curcumin. Solid lipid nanoparticles (SLNs), an emerging alternative drug delivery system, offer desirable properties such as small size, high drug loading, protection against chemical degradation, and physical stability (Gera et al., 2017). SLNs have been previously shown to increase the tissue distribution of curcumin especially in the liver and lung, and prove to be promising drug-targeting carrier into the lungs (Wang et al., 2012). However, the potential effects of curcumin-loaded SLNs (curc-SLNs) in virus-mediated asthma exacerbations is not known. Therefore, the present study was aimed to investigate the beneficial potential of curcumin-loaded SLNs in poly (I:C)-mediated exacerbation of allergic asthma, followed by an attempt to study the underlying molecular mechanisms using mouse model of the disease.

2. Materials and methods

2.1. Materials

All the chemicals used in the current study were of analytical grade. Ovalbumin (OVA) (#A5503), Aluminium hydroxide ($Al(OH)_3$) (#A1577), Poly (I:C) (#P1530), Bovine Serum Albumin (BSA) (#85171), dexamethasone (#D1756), methacholine chloride (MeCh) (62511) was purchased from Sigma Aldrich Co. (St. Louis, MO, USA). Trizol and iScript cDNA synthesis kit used for RNA isolation and cDNA preparation, Precision Plus Protein Dual color ladder (17–0374), Nitrocellulose membrane (#1620115), western ECL reagent (#170–5060) were obtained from Bio-rad, Hercules, CA, USA. Tris (#103133), Acrylamide (#193982), Glycine (#194825), and SDS (#811034) were purchased from MP Biomedicals, India. The oligonucleotide primers for qRT-PCR were purchased from Integrated DNA Technology Inc. (Coralville, Iowa, USA). Antibodies against phospho-p38MAPK (#9211S), total p38MAPK (#9212S), Nrf2 (#12721S) for western blotting were purchased from Cell Signalling Technology, Danvers, MA, USA. Antibody against β-Actin (#sc-1616) was purchased from Santa Cruz Biotechnology, USA. Curcumin extract was purchased from Sunpure Extracts Private Limited. All other reagents required in the study were purchased from HiMedia Laboratories, Mumbai, India, and Sisco Research Laboratories Pvt. Ltd., Mumbai, India.

2.2. Development of curcumin-loaded solid lipid nanoparticles

Curc-SLNs were prepared as previously reported by us (Sandhu et al., 2021). Briefly, curc-SLNs were prepared by hot high-pressure homogenization method. Curcumin (0.6% w/w) was dissolved in polyethylene glycol (PEG) 600 followed by molten Compritol® 888 ATO. This hot lipid phase was emulsified with aqueous surfactant phase containing Tween 80 and soya lecithin and maintained at a temperature 5–10 ℃ above melting point of Compritol® 888 ATO (70℃ to 75℃). This emulsion was subjected to high pressure homogenization and then allowed to cool to room temperature leading to formation of lipid nanoparticles by re-crystallization of hot dispersed lipid.

2.3. Characterization of curc-SLNs

2.3.1. Particle size and Polydispersity index (PDI)

The average particle size and PDI of curc-SLN dispersion was analyzed following appropriate dilution with distilled water (1:20) using a Delsa™ Nano C Particle Analyzer (Beckman Coulter, Brea, CA, USA).

2.3.2. Zeta Potential

Zeta potential was determined by Delsa™ Nano C Particle Analyzer (Beckman Coulter, Brea, CA, USA) after appropriate dilution with double distilled water.

2.3.3. Entrapment Efficiency

The entrapment efficiency of the prepared curc-SLNs dispersion was determined by using a dialysis membrane having pore size of 2.4 nm, and molecular weight cut-off 12–14 kDa. Membrane was soaked in double-distilled water for 12 h prior to use. The SLNs dispersion (1 ml) was placed in this pre-soaked dialysis tubing, which was hermetically sealed, and dialyzed against methanol (50 ml) at room temperature for 45 min. The amount of drug released into the receptor/release medium was spectrophotometrically analyzed with appropriate dilutions. The SLNs retained in the dialysis bag were disrupted using mixture of chloroform and methanol (1:1) to calculate the amount of drug entrapped within curc-SLNs. Entrapment efficiency was calculated using following expression.

$$\text{Entrapment efficiency (\%)} = \frac{\text{Entrapped drug content (mg)}}{\text{Actual drug content (mg)}} \times 100$$

2.4. Animal acquisition

Female BALB/c mice (4–5 weeks old) weighing around 25–30 g used in the study were obtained from Central Animal House, Panjab University, Chandigarh. Mice were housed in pathogen-free polypropylene cages under 12 h light/dark cycle and fed standard pellet diet and water ad libitum. Animals were acclimatized to local environment for one week prior to the start of the experiments. All animal experiments were carried in accordance with the ARRIVE guidelines, and the National Institutes of Health Guide for the Care and Use of Laboratory Animals (NIH Publications No. 8023, revised 1978). All animal experiments were approved by the Panjab University Institutional Animal Ethics Committee (IAEC) (Approval no: PU/45/99/CPCSEA/IAEC/2022/695).

2.5. Experimental design

Mice were randomly segregated into the following groups (n = 4–6 mice/group).

2.5.1. Group I: Control group

Mice were administered normal saline intraperitoneally followed by intranasal challenge thrice without giving any other kind of treatment.

2.5.2. Group II: [OVA + pIC] group

Mice were administered intraperitoneal injection containing 10 μg OVA adsorbed to 2 mg $Al(OH)_3$ on days 0 and 14 and then challenged with 3% aerosolized OVA using an automated exposure system (inExpose, SCIREQ Scientific Respiratory Equipment Inc., Montréal, Canada) on days 28, 29, and 30. Twenty-four hours after the last OVA challenge, mice were intranasally instilled with poly (I:C) at a dose of 200 μg under 5% isoflurane anaesthesia for three consecutive days starting on day 31 as reported by us previously (Sandhu and Naura, 2026) **(**Fig. 1**A).**

2.5.3. Group III: [OVA + pIC + Curcumin-loaded SLNs] group

OVA-sensitized and challenged mice were orally administered curcumin-loaded SLNs at different doses (0, 5, 10, or 20 mg/kg *b.wt.*) 1 h prior to each poly (I:C) instillation daily for three consecutive days **(**Fig. 1**B).**

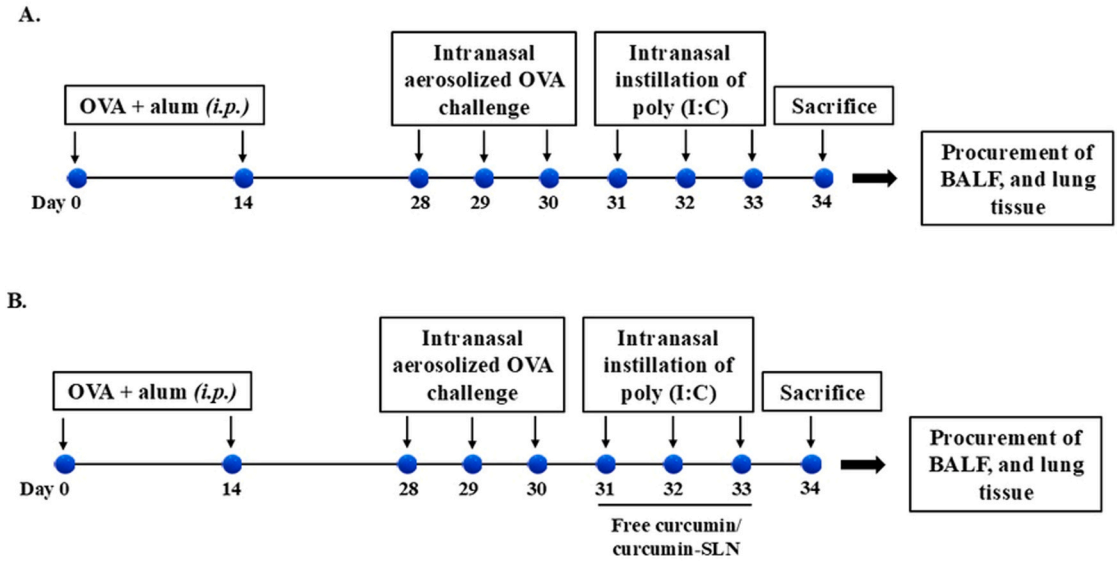


Fig. 1. Experimental protocol for curc-SLN treatment in poly (I:C)-induced asthma exacerbation. (A) Female BALB/c mice were sensitized by intraperitoneal injection containing mixture of OVA and aluminium hydroxide and then intranasally challenged with 3% aerosolized OVA on days 28, 29, and 30. Poly (I:C) was administered intranasally for three consecutive days starting 24 h after last OVA challenge. (B) Free curcumin (20 mg/kg *b.wt.*)/curcumin-loaded SLNs were orally administered one hour before each poly (I:C) instillation at different doses i.e. 0, 5, 10, or 20 mg/kg *b.wt.* On day 34, mice were sacrificed and BALF was procured for analysis of inflammatory cells and assessment of proinflammatory cytokines. Further, lung tissue was subjected to western blot/PCR/histopathological analysis.

2.5.4. Group IV: [OVA + pIC + Free curcumin] group

Free curcumin was dissolved in 0.5% carboxymethylcellulose (CMC) and orally administered at a dose of 20 mg/kg *b.wt.*1 h prior to each poly (I:C) instillation daily for three consecutive days to OVA-sensitized and challenged mice **(**Fig. 1**B)**.

2.6. Measurement of Airway Hyperresponsiveness

sRaw, a measure of airway hyperresponsiveness (AHR) was assessed in conscious mice after 24 h of the last poly (I:C) exposure using a double-chamber body plethysmograph (DCP) (SCIREQ, EMKA Technologies; Montreal, Canada). The animals were exposed to increasing concentrations of methacholine (0, 12.5, 25, and 50 mg/ml) for three minutes, after which mean readings were recorded for five minutes.

2.7. Bronchoalveolar lavage fluid (BALF) analysis

Twenty-four hours following the last poly (I:C) challenge, mice were euthanized by cervical dislocation. A small incision was made on trachea to insert a cannula and the lungs of mice were lavaged with 1 ml of ice-cold phosphate buffer saline (PBS) to procure BALF. The collected BALF was then centrifuged at 1500 rpm for 5 min at 4℃. The resulting cell pellet was resuspended in PBS to determine total number of inflammatory cells using a hemocytometer. BALF cytospin slides were prepared using cytospin centrifuge and hematoxylin and eosin (H&E) stained slides were used for differential analysis of inflammatory cells as previously reported (Puri and Naura, 2020).

2.8. RNA extraction and real-time PCR

Total RNA was extracted from the lung tissues preserved in RNA later using Trizol reagent as per the manufacturer's instructions. The concentration and purity of RNA were evaluated with a nanodrop spectrophotometer while its integrity was checked by agarose gel electrophoresis. 1 μg of RNA from each sample was reverse transcribed to cDNA using the iScript cDNA synthesis kit (Biorad, Hercules, USA). The resulting cDNA was used in combination with SYBR green to quantify the expression of genes namely TNF-α, IL-6, G-CSF (granulocyte colony stimulating factor), KC (keratinocyte-derived chemokine), and β-actin using specific primers as mentioned in Table 1**.** Quantitative real-time PCR was conducted using CFX 96 Real Time System, Biorad, Hercules, USA) as previously reported (Chandel and Naura, 2025).

2.9. Histopathological analysis

The lungs of mice inflated using 10% neutral buffered formalin (prepared in PBS) were harvested and kept in 10% formalin for the next 24 h. Following this, the tissues were embedded in paraffin blocks and tissue sections of 5 μm were prepared and fixed onto microscopic slides. These paraffin-embedded tissue slides were then subjected to H&E staining for inflammatory cells and periodic acid-Schiff (PAS) staining for mucus production respectively. Multiple images of H&E-stained and PAS-stained slides were captured at 100X and 400X. Histological inflammation score was calculated by the degree of peribronchial and perivascular inflammation, evaluated on a scale of 0–4: 0 (normal), 1 (occasional cuffing with inflammatory cells), 2 (most bronchi or vessels surrounded by a depth of 1–3 cells), 3 (most bronchi or vessels surrounded by a depth of 4–5 cells), 4 (most bronchi or vessels surrounded by a depth of >5 cells). Peribronchial inflammation was evaluated for severity based on scoring system (0: normal, 1: diameter of <3 cells thick, 2: diameter of 3–10 cells thick, 3: diameter of >10 cells thick) and extent (with a score of 0: normal, 1: <10% of the sample, 2: 10–25% of the sample, 3: >25% of the sample). Inflammation scores were calculated by multiplying severity by extent (Gracias et al., 2021). PAS-stained lung sections were used for counting of goblet cells using an arbitrary scoring system (0: <5% goblet cells; 1: 5–25%; 2: 25–50%; 3: 50–75%; 4: >75%), as described by Grunig et al (Grünig et al., 1998).

Table 1
List of primers used in the experimental study.

Gene	Forward Primer 5′-3′	Reverse Primer 3′-5′
TNF-α	TAT GGC TCA GGG TCC AAC TC	CTC CCT TTG CAG AAC TCA GG
IL-6	CCG GAG AGG AGA CTT CAC AG	TCC ACG ATT TCC CAG AGA AC
G-CSF	CCT TCA CTT CTG CCT TCC AG	GCT CAG GTC TAG GCC AAG TG
KC	GCT GGG ATT CAC CTC AAG AA	TCT CCG TTA CTT GGG GAC AC

2.10. Western Blotting

Total protein extracted from lung tissue was lysed in ice-cold RIPA buffer containing protease and phosphatase inhibitors. The protein lysates were centrifuged to collect supernatant which was used to determine the protein concentration by Bradford assay (Bradford, 1976). 40 μg protein from each sample was separated on 10% SDS-PAGE and then transferred to nitrocellulose membrane. The membranes were blocked with 3% BSA for 1 h at room temperature, and then incubated with primary monoclonal antibodies against β-Actin (1:1000), phospho (Thr^{180}/Tyr^{182})-p38MAPK (1:1000), total p38MAPK (1:1000), and Nrf2 (1:1000) overnight at 4℃. After washing the membrane with PBS-T (PBS with 0.05% Tween-20) thrice, membranes were subsequently incubated with suitable horseradish peroxidase (HRP)-conjugated secondary antibody (1:10,000). The blots were finally visualised via chemiluminescence with the ECL-Plus (Bio-Rad, Hercules, CA, USA) using Image QuantTM LAS 500 (GE Healthcare Life Sciences). Densitometric analysis was performed using Image J software and protein expression was normalized against β-actin.

2.11. Biochemical Parameters

The lung tissue homogenates (10% w/v) were prepared in ice-cold PBS (0.1 N, pH 7.4) at 4°C using a Potter/Elvehjem homogenizer and was centrifuged at 8000 rpm for 10 min to collect supernatant. The levels of ROS, malondialdehyde (MDA), reduced glutathione (GSH), and superoxide dismutase (SOD) activity were determined in the lung tissue homogenates as described previously (Kaur et al., 2024).

2.12. Statistical analysis

Results are depicted as mean ± SD. Since the data were normally distributed, parametric analysis were performed by using one way analysis of variance (ANOVA), followed by Tukey's multiple comparisons using Graph-pad prism software (GraphPad Software, Inc. La Jolla, CA). sRaw was analyzed using two-way ANOVA followed by Tukey's multiple comparisons post-test. p value of < 0.05 or less was considered as statistically significant.

3. Results

3.1. Development and characterization of curc-loaded SLNs

3.1.1. Particle size and PDI

The mean particle size of curc-SLNs was observed to be **147.5 ± 19.15** with a PDI of **0.316 ± 0.056** (n = 6), indicating a narrow particle size distribution while the mean particle size of blank SLNs was found to be **134.69 nm** with a PDI of **0.176 (**supplementary figure **1)**. It is evident that incorporation of curcumin did not significantly alter the particle size of the nanoparticles. The small particle size obtained with both blank and curc-loaded SLNs may be attributed to the presence of satisfactory surfactant and co-surfactant concentration resulting in reduction of the surface tension and production of small-size particles. Further, a low PDI indicates uniform distribution of particles around the mean.

3.1.2. Zeta potential

Zeta potential of curc-SLNs was measured by Delsa Nano C Zetasizer (Beckman Coulter, Brea, CA, USA) at 25°C and was found to be **-8.816 ± 0.610** (n = 6) **(**supplementary figure **2)**. High negative charge indicates formation of stable nano-particulate system with lower chances of aggregation post-storage for prolonged time period. The negative charge can be associated with the presence of hydroxyl ions on the surface of the lipid nanostructures and is consistent with the observations in the previous studies.

3.1.3. Morphology and entrapment efficiency

The FESEM and TEM of curc-SLNs showed spherical particles without any presence of agglomerates indicating their stability as reported by us previously (Sandhu et al., 2021). The entrapment efficiency of these prepared curc-SLNs was observed to be **80.1 ± 0.26%**. The higher entrapment efficiency indicates that the method used for the preparation of curc-SLNs is suitable and reliable.

The characterization of curc-SLN confirms that curc-SLN were successfully formulated with optimal particle size, sufficient surface charge, and optimal entrapment efficiency. The efficacy of curc-SLNs was further tested under the experimental conditions mimicking virus-mediated asthma exacerbation.

3.2. Curcumin mitigates the poly (I:C) mediated neutrophilic inflammation and airway hyperresponsiveness in OVA-exposed mice

Curcumin at a dose of 20 mg/kg *b.wt.* has been reported to show beneficial potential in allergic asthma and associated exacerbations (Yang et al., 2017; Kumari et al., 2015). In line with this, we initially tested the efficacy of free curcumin under the conditions of poly (I:C) mediated asthma exacerbations. Curcumin was orally administered at a dose of 20 mg/kg *b.wt.* before poly (I:C) instillation in OVA-exposed mice. A steep increase in the inflammatory cells (~11 folds, $p < 0.001$) was observed in the BALF of OVA + poly (I:C) exposed mice compared to the control mice **(**Fig. 2**A)**. Quantitative analysis of BAL cells confirmed that neutrophils were the majority of inflammatory cells recruited upon combined exposure to OVA + poly (I:C). Pretreatment with curcumin markedly blunted the infiltration of neutrophils (~1.9 folds, $p < 0.01$) in the lungs of mice subjected to OVA + poly (I:C) treatment **(**Fig. 2**B and C)**. Further, in our recent study we have reported that poly (I:C) mediated asthma exacerbation is associated with elevated sRaw which is an indicator of airway hyperresponsiveness. As shown in Fig. 2**D,** curcumin significantly mitigated the OVA + poly (I:C) mediated increase in sRaw in response to increasing concentrations of methacholine (12.5, 25, and 50 mg/ml).

Overall, these findings suggest that curcumin possesses anti-inflammatory properties as it effectively ameliorates neutrophilic inflammation and AHR in OVA + poly (I:C) exposed mice. Based on these observations, but due to poor solubility and limited bioavailability, we next investigated whether curcumin in the form of solid lipid nanoparticles could further enhance its potency under these conditions.

3.3. Oral administration of curcumin-loaded SLN alleviates infiltration of inflammatory cells in the lungs of mice subjected to poly (I:C)-mediated asthma exacerbation

The infiltration of inflammatory cells, primarily neutrophils, in the lungs is a key feature of virusinduced asthma exacerbation. Thus, we first examined the potential of curc-SLN to counter the influx of inflammatory cells in the lungs of mice subjected to asthma exacerbation using a combination of OVA and poly (I:C). It is evident that intranasal poly (I:C) instillation in OVA-sensitized and challenged mice caused a substantial increase in the total inflammatory cells (~11 folds, $p < 0.001$) in the BALF in comparison to the control mice. Oral administration of curc-SLN at a dose of 5 mg/kg b.wt. to mice subjected to OVA + poly (I:C) treatment was unable to ameliorate the inflammatory cells significantly. However, increasing the dose to 10 mg/kg and 20 mg/kg resulted in reduction in total number of inflammatory cells in the BALF by 2 folds and 3 folds respectively **(**Fig. 3**A)**. Differential qualitative and quantitative analysis of BALF cytospin slides revealed that the majority of inflammatory cells recruited in the lungs of OVA + poly (I:C) exposed mice were neutrophils, which were markedly reduced by prior treatment with curc-SLNs, particularly at dose regimens of 10 mg/kg (~2.5 folds, $p < 0.001$) and 20 mg/kg (~4.5 folds, $p < 0.001$) **(**Fig. 3**B and C)**.

Histopathological analysis of H&E-stained lung tissue sections

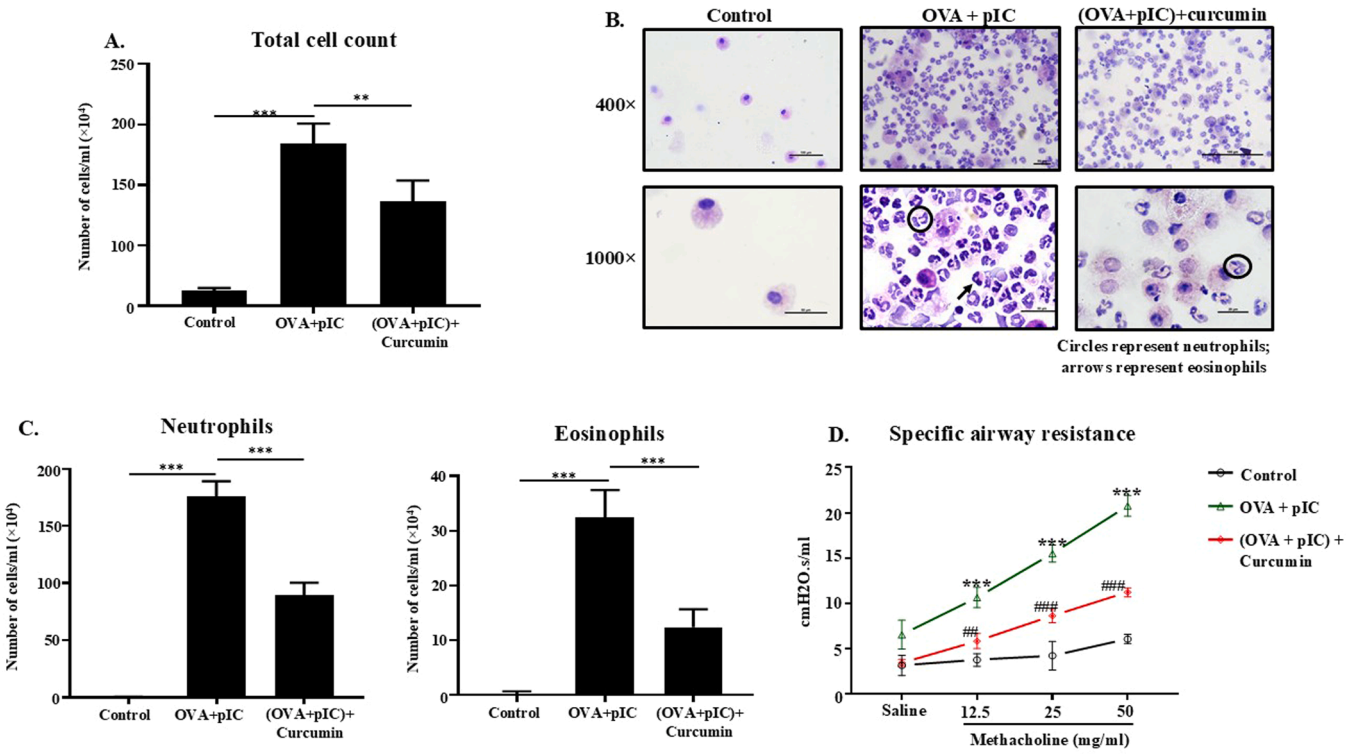


Fig. 2. Curcumin administration in OVA + poly (I:C) exposed mice is associated with attenuation of neutrophilic inflammation and AHR. OVA-sensitized and challenged mice were instilled with poly (I:C) to induce phenotype of asthma exacerbation. Curcumin was administered orally one hour prior to each poly (I:C) instillation and BALF was collected to assess (A) Total inflammatory cells; (B) Representative images of H&E-stained BALF cytoslides from different experimental groups; (C) Quantitative analysis showing neutrophils and eosinophils; (D) sRaw plotted against increasing concentrations of methacholine. Data is represented as mean ± SD (n = 4–5 animals/group). Statistical analysis was performed by one-way ANOVA followed by Tukey's multiple comparisons. **p < 0.01, ***p < 0.001, $^{\#}$p < 0.01 w.r.t. OVA + pIC, $^{\#,\#,\#}$p < 0.001 w.r.t. OVA + pIC. pIC: poly (I:C).

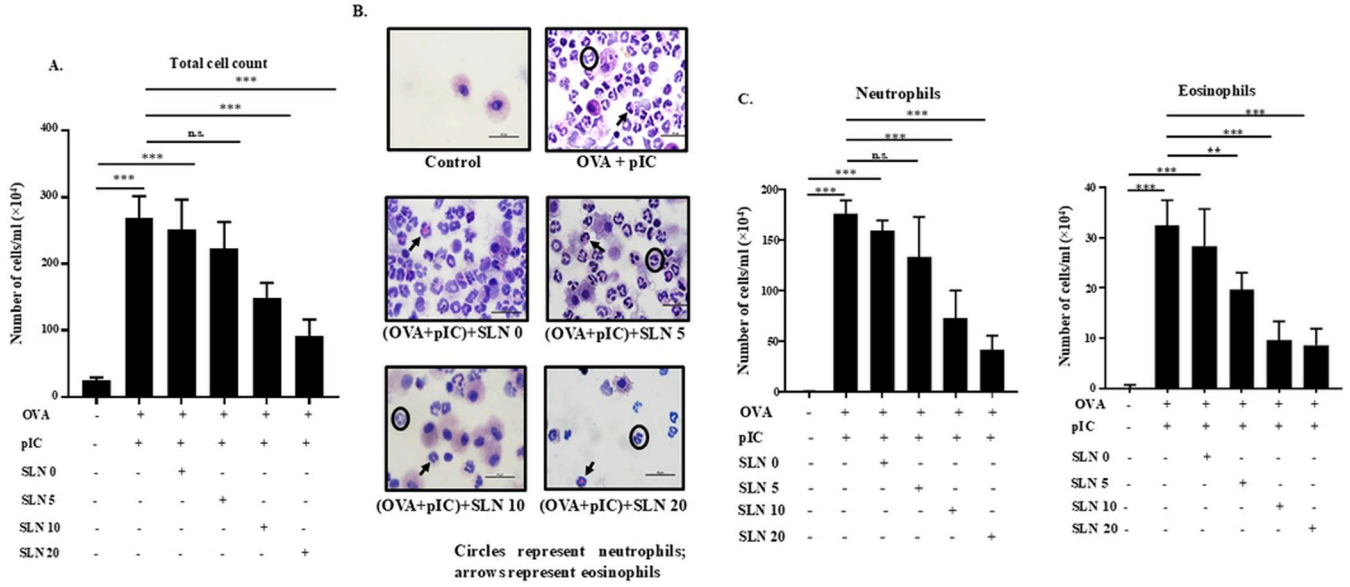


Fig. 3. Curcumin-loaded SLN ameliorated lung inflammation in poly (I:C)-mediated asthma exacerbation. OVA-sensitized and challenged mice were instilled with poly (I:C) to induce phenotype of asthma exacerbation. Curc-SLN were administered orally one hour prior to each poly (I:C) instillation and subjected to procurement of BALF and lung tissues for the assessment of (A) Total inflammatory cell count; (B) Representative images of H&E-stained BALF cytoslides from different experimental groups; (C) Quantitative analysis of showing neutrophils and eosinophils. Data is represented as mean ± SD (n = 4–5 animals/group). Statistical analysis was performed by one-way ANOVA followed by Tukey's multiple comparisons. **p < 0.01, ***p < 0.001, n.s. non-significant. pIC: poly (I:C), SLN 0: curcumin-loaded SLN (0 mg/kg), SLN 5: curcumin-loaded SLN (5 mg/kg), SLN 10: curcumin-loaded SLN (10 mg/kg), SLN 20: curcumin-loaded SLN (20 mg/kg).

confirmed that poly (I:C) instillation in OVA-exposed mice led to significant inflammatory cell recruitment around the bronchi. On the other hand, oral administration of curc-SLN (10 mg/kg and 20 mg/kg) reduced the infiltration of inflammatory cells with maximum effect

observed at a dose of 20 mg/kg **(**Fig. 4**A and B)**. Overall, the data revealed that administration of curc-SLN at 20 mg/kg *b.wt.* (equivalent to that of free curcumin) showed much better effects in ameliorating the poly (I:C) mediated neutrophilic inflammation while even the lower dose i.e. 10 mg/kg *b.wt.* achieved comparable effects to that of a double dose of 20 mg/kg *b.wt.* of free curcumin. Additionally, to compare the impact of curc-SLN with dexamethasone, a steroid class of drugs, BAL cells procured from mice subjected to different treatments were quantified. The data demonstrated that while dexamethasone failed to ameliorate the recruitment of inflammatory cells, particularly neutrophils in the lungs of OVA + poly (I:C) exposed mice but curc-SLNs ameliorated the inflammation in OVA + poly (I:C) exposed mice substantially, confirming the protective efficacy of curc-SLNs even under steroid resistance conditions in our model **(**supplementary figure **3)**.

Further to confirm, if nanocarrier alone can cause any effect on inflammatory response, a comparative analysis of control group of mice was done with blank-SLNs group where naïve mice were orally administered blank-SLNs (without drug) for three consecutive days (once daily). Our data demonstrated that blank-SLNs alone did not cause any alteration in the total cells in the BALF in comparison to the control group, confirming non-visible effect on inflammatory/immune response (supplementary figure **4).**

3.4. Pre-treatment of curcumin-loaded SLN was associated with normalization of airway hyperresponsiveness in OVA + poly (I:C) exposed mice

Acute asthma exacerbations are associated with reduced airflow resulting mainly from increased airway resistance (Bakakos et al., 2023). Therefore, we analyzed the effect of curc-SLN on OVA + poly (I:C)-mediated airway hyperresponsiveness in asthmatic mice. Data revealed that OVA + poly (I:C)-exposed mice showed significant increase in sRaw, a measure of airway hyperresponsiveness, with increasing concentrations of methacholine as compared to control mice. Pre-treatment with curc-SLNs at a dose of 5 mg/kg was unable to cause much improvements in sRaw when exposed to increasing concentrations of methacholine. Notably, oral administration of curc-SLN to OVA + poly (I:C)-exposed mice at the doses of 10 mg/kg and 20 mg/kg was associated with significant improvements in sRaw towards normal in comparison to OVA + poly (I:C) exposure, with maximal benefit at 20 mg/kg **(**Fig. 5**)**. The above data demonstrated that curc-SLNs ameliorated OVA + poly (I:C) mediated airway hyperresponsiveness in mice.

3.5. Curcumin-loaded SLN mitigated OVA + poly (I:C) induced mucus overproduction in the lungs of mice

Because mucus hypersecretion is an important hallmark feature of asthma, we investigated the effect of curc-SLN on mucus hypersecretion

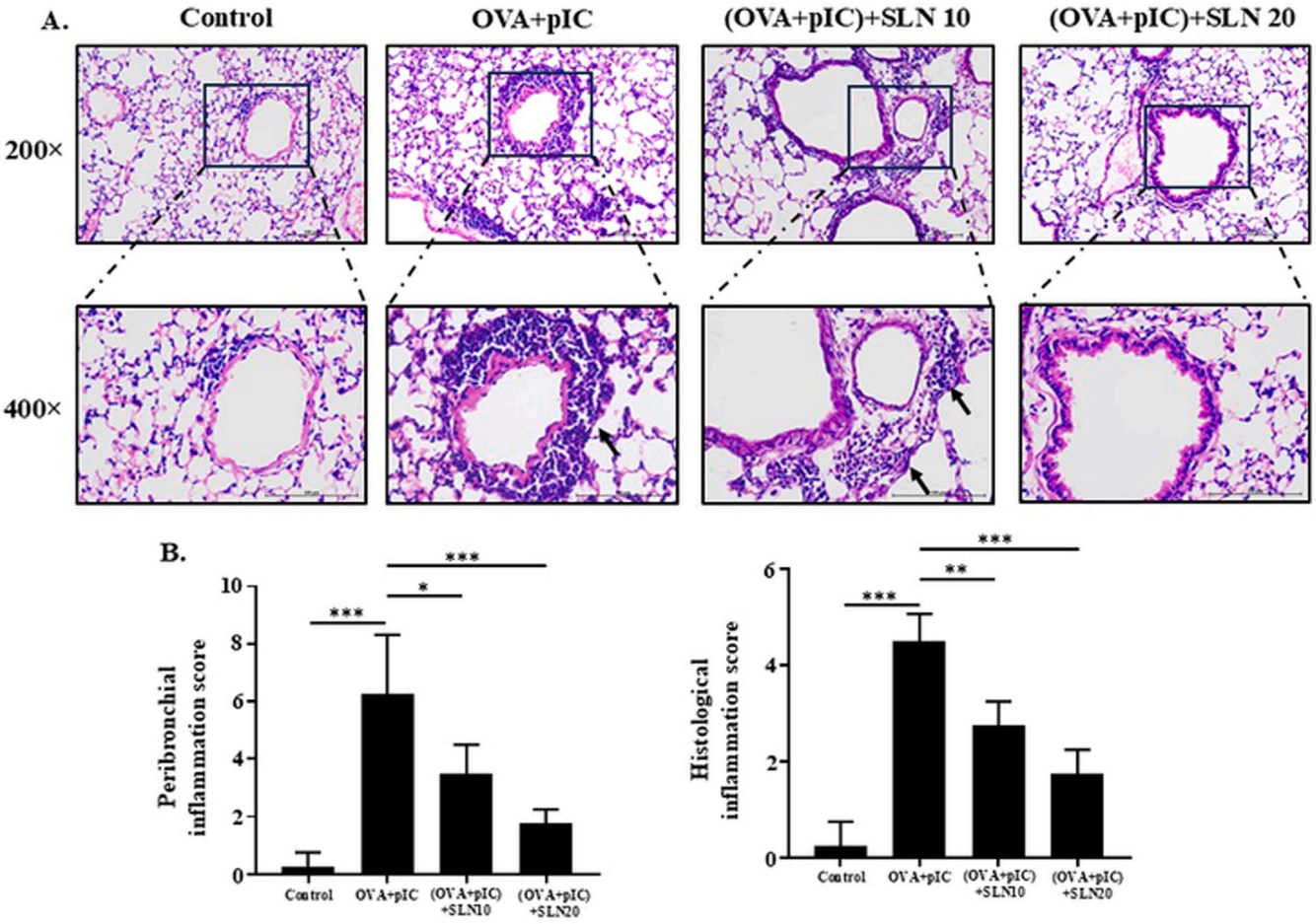


Fig. 4. Histological assessement of lung tissues following oral administration of curc-SLNs. (A) H&E-stained histological sections of lung tissues showing inflammatory cells recruitment at a magnification of 200 × and 400 × . (B) Peribronchial inflammation score and histological inflammation score. Data is represented as mean ± SD (n = 4 animals/group). Statistical analysis was performed by one-way ANOVA followed by Tukey's multiple comparisons. *p < 0.05, **p < 0.01, ***p < 0.001. pIC: poly (I:C), SLN 10: curcumin-loaded SLN (10 mg/kg), SLN 20: curcumin-loaded SLN (20 mg/kg).

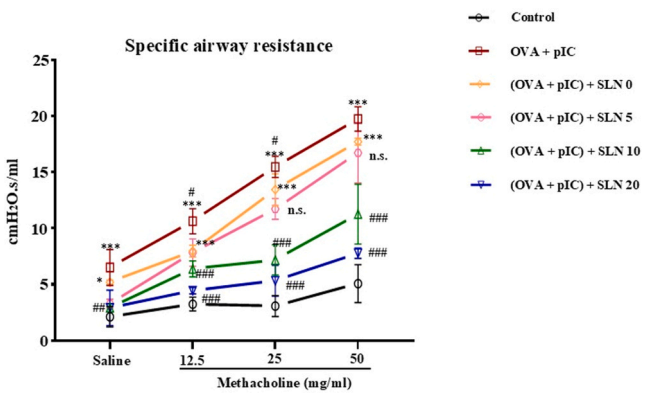


Fig. 5. Effect of curcumin-loaded SLN on sRaw in poly (I:C)-mediated asthma exacerbation mice. Twenty-four hours after last poly (I:C) challenge, mice were exposed to increasing concentrations of methacholine followed by plethysmography. sRaw showed normalization towards basal level upon pretreatment with curc-SLN in a dose-dependent manner. Data is represented as mean ± SD (n = 3 animals/group). Statistical analysis was performed by one-way ANOVA followed by Tukey's multiple comparisons. *$p < 0.05$ w.r.t. control, ***$p < 0.001$ w.r.t. control, $^{\#}p < 0.05$ w.r.t. OVA + pIC, $^{\#,\#}p < 0.01$ w.r.t. OVA + pIC, $^{\#,\#,\#}p < 0.001$ w.r.t. OVA + pIC, n.s. non-significant. pIC: [poly (I:C)]), SLN 0: curcumin-loaded SLN (0 mg/kg), SLN 5: curcumin-loaded SLN (5 mg/kg), SLN 10: curcumin-loaded SLN (10 mg/kg), SLN 20: curcumin-loaded SLN (20 mg/kg).

in OVA + poly (I:C) treated mice. Histopathological analysis of PAS-stained lung tissue sections revealed a substantial increase in mucus production in the lungs tissue sections of OVA and poly (I:C)-exposed mice. In contrast, oral administration of curc-SLN markedly ameliorated the mucus production at both the doses i.e. 10 mg/kg and 20 mg/kg (Fig. 6**A**). Additionally, mucus overproduction is correlated to airflow limitation. Therefore, we also examined the effect of curc-SLN on peak expiratory flow (PEF), a measure of airflow limitation. Pre-treatment of OVA + poly (I:C) treated mice with curc-SLN showed significant improvements in PEF at 10 mg/kg and 20 mg/kg with better observations at higher dose (Fig. 6**B**).

3.6. Curcumin-loaded SLNs downregulated the expression of inflammatory mediators upon exposure to OVA + poly (I:C) in mice

Several cytokines are released by inflammatory cells that mediate recruitment, activation, and survival of these inflammatory cells during the orchestration of asthma. Although, asthma is dominated by T_H2 immune response, our previous study showed that T_H2 response was comparatively subdued but surprisingly innate immune response was found to be prominently activated upon poly (I:C) mediated asthma exacerbation. Therefore, we next performed qRT-PCR to analyze the effect of curc-SLN at a dose of 20 mg/kg b.wt. on these inflammatory mediators namely TNF-α, IL-6, G-CSF, and KC. Fig. 7 revealed that OVA + poly (I:C) showed a steep increase in the mRNA expression of inflammatory mediators specifically TNF-α (~4 folds, $p < 0.01$), IL-6 (~5 folds, $p < 0.01$), G-CSF (~10 folds, $p < 0.01$), and KC (~15 folds, $p < 0.001$). Pre-treatment with curc-SLN at a dose of 20 mg/kg markedly reduced the expression of TNF-α (~ 3.5 folds, $p < 0.01$), IL-6 (~5 folds, $p < 0.01$), G-CSF (~6 folds, $p < 0.01$), and KC (~6.5 folds, $p < 0.01$) in the lungs of OVA + poly (I:C) exposed mice towards normal **[**Fig. 7 **(A-D)]**.

3.7. Curcumin-loaded SLN ameliorated OVA + poly (I:C)-mediated increase in proinflammatory mediators in the BALF of mice

Previously, we have reported that OVA + poly (I:C) mediated

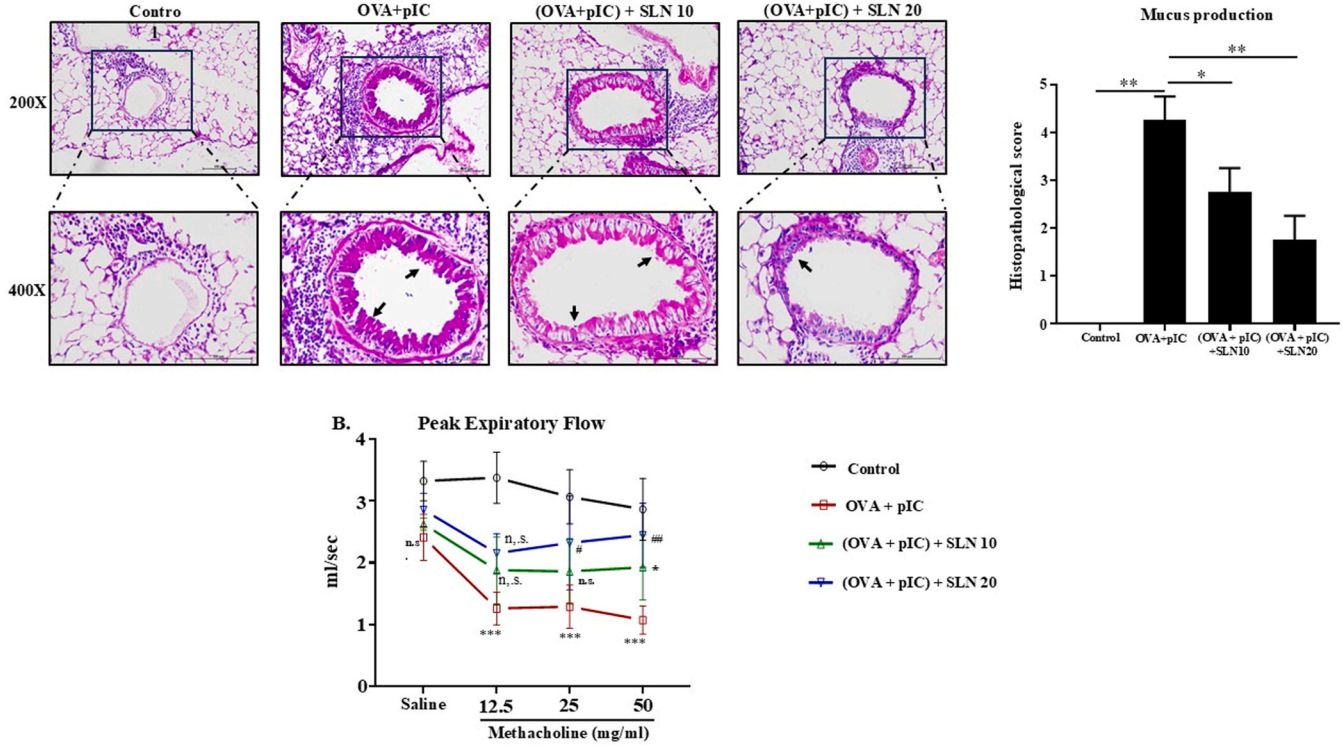


Fig. 6. Effect of curcumin-loaded SLN on mucus production in OVA + poly (I:C)-mediated asthma exacerbation in mice. (A) Lung tissue sections stained with PAS were observed under a light microscope (200 × and 400 ×) to detect PAS-positive goblet cells. Arrows represent PAS-positive mucus cells. (B) PEF, measure of airflow limitation, was plotted against increasing concentrations of methacholine. Data is represented as mean ± SD (n = 3 animals/group). Statistical analysis was performed by one-way ANOVA followed by Tukey's multiple comparisons. *$p < 0.05$ w.r.t. control, ***$p < 0.001$ w.r.t. control, $^{\#}p < 0.05$ w.r.t. OVA + pIC, $^{\#,\#}p < 0.01$ w.r.t. OVA + pIC, n.s. non-significant. pIC: poly (I:C), SLN 10: curcumin-loaded SLN (10 mg/kg), SLN 20: curcumin-loaded SLN (20 mg/kg).

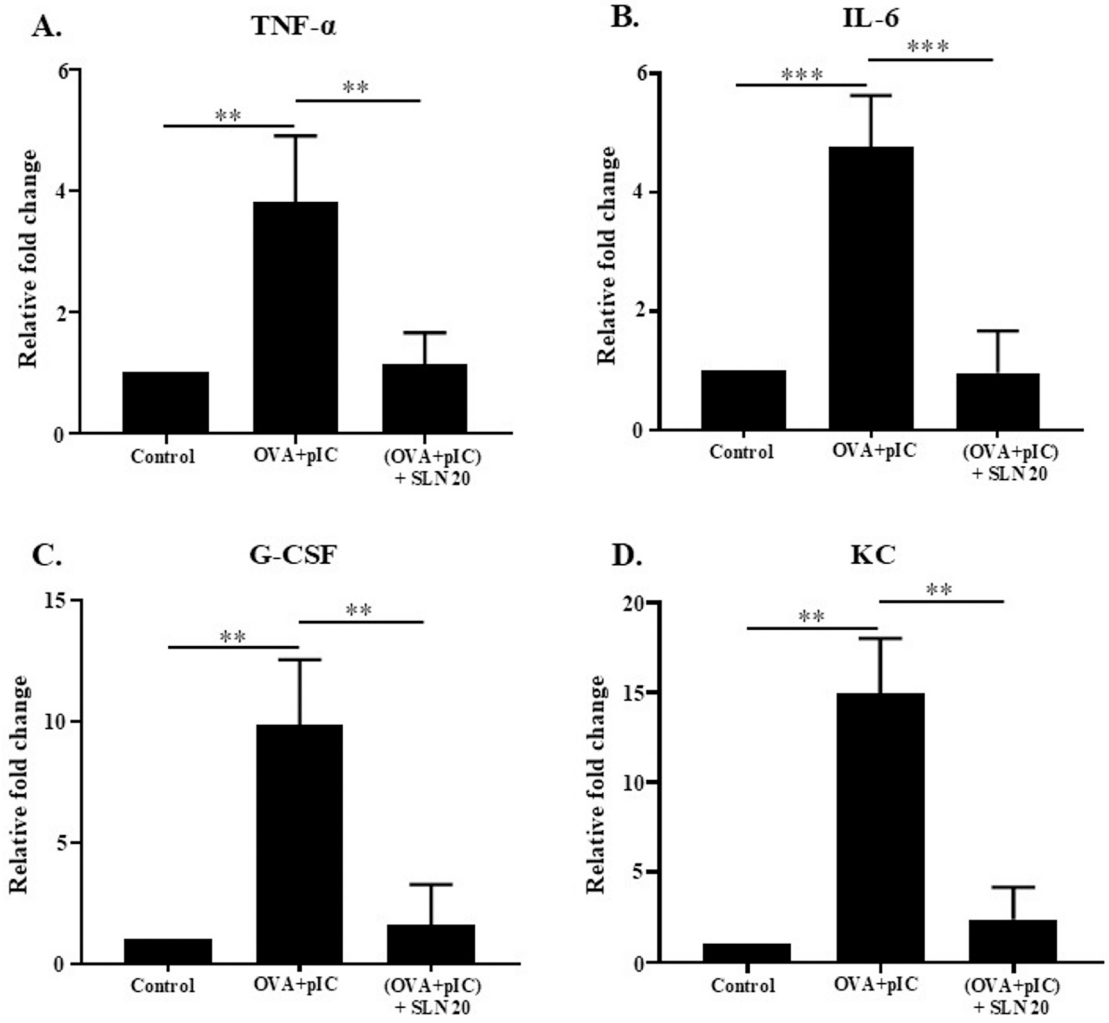


Fig. 7. Effect of curcumin-loaded SLN on gene expression of inflammatory mediators in OVA + poly (I:C)-mediated asthma exacerbation in mice. cDNA prepared from the isolated RNA was subjected to qRT-PCR for the analysis of gene expression of inflammatory mediators (A) TNF-α; (B) IL-6; (C) G-CSF; (D) KC. Data is represented as mean ± SD (n = 3). Statistical analysis was performed by one-way ANOVA followed by Tukey's multiple comparisons. **$p < 0.01$, and ***$p < 0.001$. pIC: poly (I:C), SLN 20: curcumin-loaded SLN (20 mg/kg).

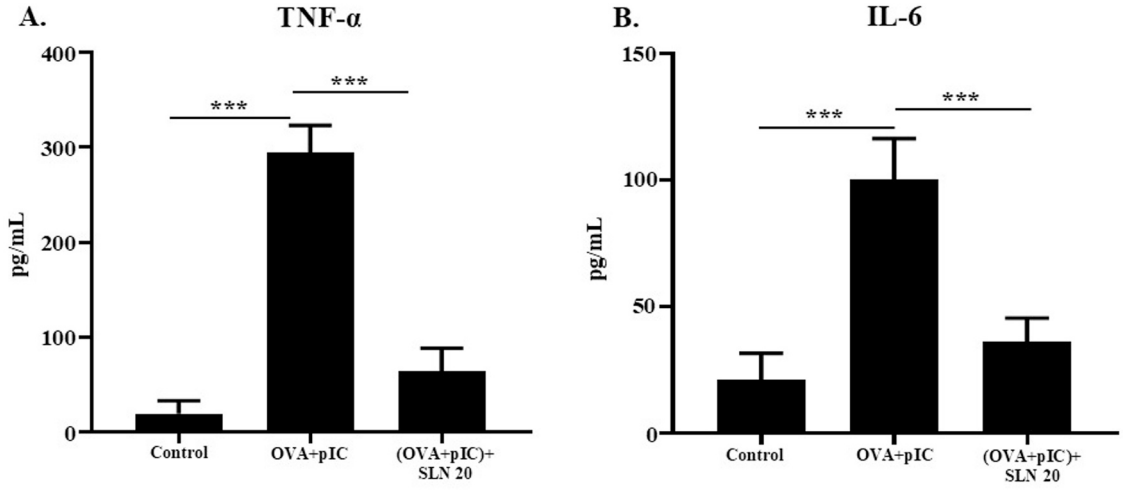


Fig. 8. Effect of curcumin-loaded SLN on protein levels of proinflammatory mediators in OVA + poly (I:C)-mediated asthma exacerbation in mice. Levels of (A) TNF-α, and (B) IL-6 were analyzed in BALF and found to be significantly reduced upon oral administration of curc-SLN in OVA + poly (I:C) exposed mice. Data is represented as mean ± SD (n = 4). Statistical analysis was performed by one-way ANOVA followed by Tukey's multiple comparisons. ***$p < 0.001$. pIC: poly (I:C), SLN 20: curcumin-loaded SLN (20 mg/kg).

asthma exacerbation was associated with steep rise in proinflammatory cytokines, particularly TNF-α and IL-6. Therefore, we next decided to analyze whether anti-inflammatory action exerted by curc-SLN are associated with production of these proinflammatory cytokines. Indeed oral pretreatment with curc-SLN led to a marked decline in the levels of both cytokines TNF-α (~4.5 folds, $p < 0.001$) and IL-6 (~2.7 folds, $p < 0.001$) in the BALF of OVA + poly (I:C) exposed mice **(**Fig. 8**A and B)**.

3.8. Curcumin-loaded SLN pre-treatment restores OVA + poly (I:C)-mediated redox imbalance in the lungs of mice

Evidence suggests that inflammatory cells release reactive oxygen intermediates that cause oxidative damage and further aggravate the lung inflammation (Pérez-Figueroa et al., 2021). It is well known that curcumin possess anti-oxidant properties, therefore, we next evaluated the effect of curc-SLNs on the redox balance in the lung tissue homogenate of OVA + poly (I:C)-exposed mice. Thus, we quantified the levels of oxidative stress parameters i.e. ROS, MDA, protein carbonyl, and GSH. It is evident that OVA + poly (I:C) treatment in mice elevated the oxidative stress markedly as reflected by the data on ROS, MDA, protein carbonyl, and GSH as compared to the control mice. Interestingly, curc-SLN at a dose of 20 mg/kg restored the levels of ROS (~2 folds, $p < 0.001$), MDA (~3 folds, $p < 0.001$), and protein carbonyl (~2.5 folds, $p < 0.001$), and GSH (~1.5 folds, $p < 0.01$) substantially towards normal in comparison to OVA + poly (I:C) exposed mice **[**Fig. 9**(A-D)]**.

3.9. Curcumin-loaded SLN administration to OVA + poly (I:C) exposed mice leads to reduced phosphorylation of p38MAPK but enhanced expression of Nrf2 in lung tissue

In light of the observed amelioration in inflammation and restoration of redox balance, we next sought to investigate whether curc-SLN modulate key upstream signalling pathways governing these responses. Therefore, western blot analysis was conducted to check the activation status of p38MAPK and the expression of antioxidant transcription factor Nrf2. Phosphorylation of MAPK at Thr^{180}/Tyr^{182} is recognized as an indicator of its activation. As expected, OVA + poly (I:C) mediated asthma exacerbation resulted in a remarkable upregulation in the phosphorylation status of p38MAPK in comparison to the control mice, confirming the activation of pro-inflammatory pathway. On the other hand, the expression of Nrf2 was observed to be markedly suppressed upon OVA + poly (I:C) treatment in mice, reflecting impaired antioxidant defence. Notably, pre-treatment with curc-SLN at dose of

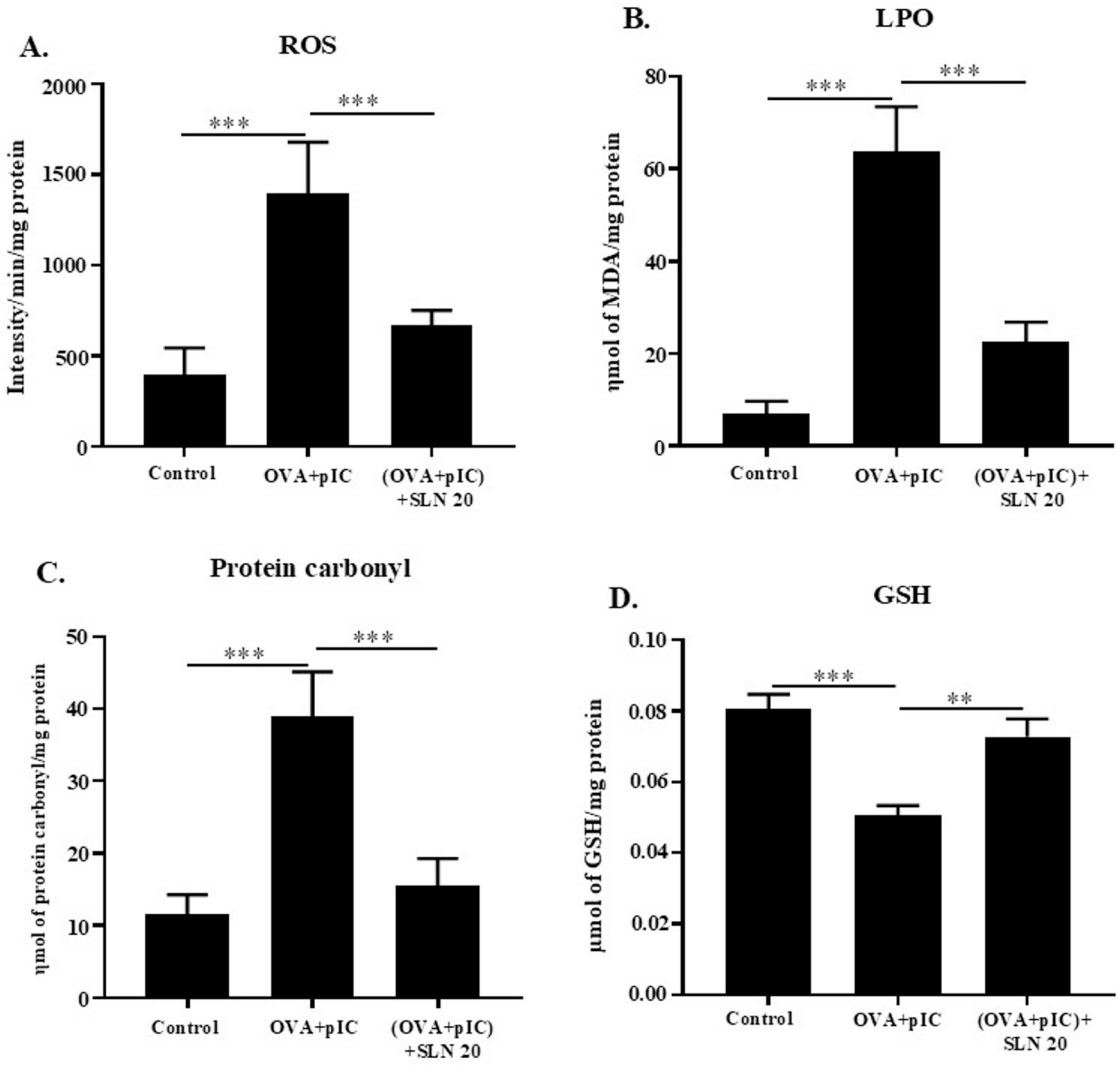


Fig. 9. Effect of curcumin-loaded SLN on oxidative stress in OVA and poly (I:C) exposed mice. Lung tissues were assessed for (A) ROS; (B) MDA; (C) Protein carbonyl; (D) GSH. Data is represented as mean ± SD (n = 4 animals/group). Statistical analysis was performed by one-way ANOVA followed by Tukey's multiple comparisons. **p < 0.01, ***p < 0.001. pIC: poly (I:C), SLN 20: curcumin-loaded SLN (20 mg/kg).

20 mg/kg significantly attenuated p38MAPK phosphorylation while restoring expression of Nrf2 back towards basal level (Fig. 10**A and B**). These results suggest that curc-SLNs exert its protective effects partly by inhibiting p38MAPK activation and reactivating Nrf2 antioxidant signalling.

4. Discussion

Viral infections are major contributors to asthma exacerbations, with nearly 80% of episodes associated with respiratory viruses (Bochkov and Gern, 2016; Nakagome and Nagata, 2022). Although corticosteroids, often combined with bronchodilators, are the cornerstone treatment for asthma, approximately 5–10% of asthmatic patients exhibit poor responsiveness to steroid-based therapies including virus-mediated asthma exacerbation, and are increasingly becoming resistant to steroid use (Wadhwa et al., 2019). This leads to increased hospitalizations and emergency department visits and account for around 50% of asthma related health care costs. Despite being the primary treatment for majority of asthma patients, the 5–10% of patients who do not respond effectively to these treatments underscore the urgent need for alternative strategies capable of targeting these sudden episodes of asthma worsening (Adcock and Ito, 2004). In this context, we investigated the protective effects of curcumin-loaded SLNs under conditions mimicking viral mediated exacerbation of allergic asthma using combination of OVA and poly (I:C).

The immune response plays a crucial role in the pathogenesis of asthma exacerbation, with infiltration of various inflammatory cells being a characteristic manifestation of airway inflammation (Mei et al., 2022). The neutrophilic inflammation is a defining feature of virus-mediated asthma exacerbations and correlates with disease severity and steroid insensitivity (Wark et al., 2001; Curren et al., 2023; Ito et al., 2008). These recruited inflammatory cells release a cascade of cytotoxic proteins, lipid mediators, ROS, and cytokines which collectively drive airway hyperresponsiveness (AHR) and mucus overproduction (Park et al., 2016). Therefore, modulating the neutrophil influx and derived mediators could be a valuable therapeutic approach in virus-mediated asthma exacerbation. Accordingly, we initially assessed the effect of curc-SLN on OVA + poly (I:C)-mediated asthma exacerbation like features. Our data confirms that OVA + poly (I:C) exposure to mice mimics asthma exacerbation like features as reflected by a massive surge in the infiltration of inflammatory cells, particularly neutrophils in lungs of mice which is in line with our recent report (Sandhu and Naura, 2026). Further, OVA + poly (I:C)-mediated influx of inflammatory cells was effectively attenuated by pretreatment with curc-SLN in a dose-dependent manner. Neutrophils, together with activated epithelial cells are a rich source of cytokines, chemokines, and growth factors that amplify the inflammatory response. Poly (I:C) robustly engages TLR3 and activates nuclear factor κB (NF-κB) signalling pathway and Mitogen-Activated Protein Kinase (MAPK) pathway which leads to heightened transcription of pro-inflammatory mediators like IL-6, IL-8, and TNF-α (Yong et al., 2009; Yang et al., 2022). The inflammatory cytokines TNF-α and IL-6 regulate inflammation through activation, and recruitment of neutrophils, promoting the neutrophil infiltration to the inflammatory sites, and triggering the release of various free radicals, therefore orchestrate the inflammatory process in asthma (Niessen et al., 2021; Kolaczkowska and Kubes, 2013). Further, the pro-inflammatory milieu created in the airways of asthmatics-characterized by elevated TNF-α and IL-6 also potentiate AHR by enhancing airway smooth muscle (ASM) responsiveness possibly via modulation of calcium signalling (Sutcliffe et al., 2012; Lai and Rogers, 2010). In agreement with these mechanisms, our qRT-PCR data indicate that curc-SLN treatment markedly blunts the OVA + poly (I:C)-mediated increased expression of TNF-α, IL-6, G-CSF, and KC in lung tissues of mice. Moreover, the protein levels of TNF-α, and IL-6 in BALF were found to be remarkably reduced following curc-SLN treatment in OVA + poly (I:C)-mediated asthma exacerbations. Such suppression in cytokine expression/production was mirrored by physiological improvements as substantial reduction in sRaw was observed. Further the histopathological data reveals that curc-SLN effectively mitigated the OVA + poly (I:C) mediated mucus overproduction. The above findings align with previous studies demonstrating the anti-inflammatory properties of curcumin against various inflammatory diseases like allergic asthma, COPD, inflammatory bowel disease, acute pancreatitis, arthritis, atherosclerosis (Burge et al., 2019; Xu et al., 2022; Wang et al., 2019; Shahid et al., 2019). Mechanistically, curcumin's anti-inflammatory effects are strongly linked to its ability to inhibit

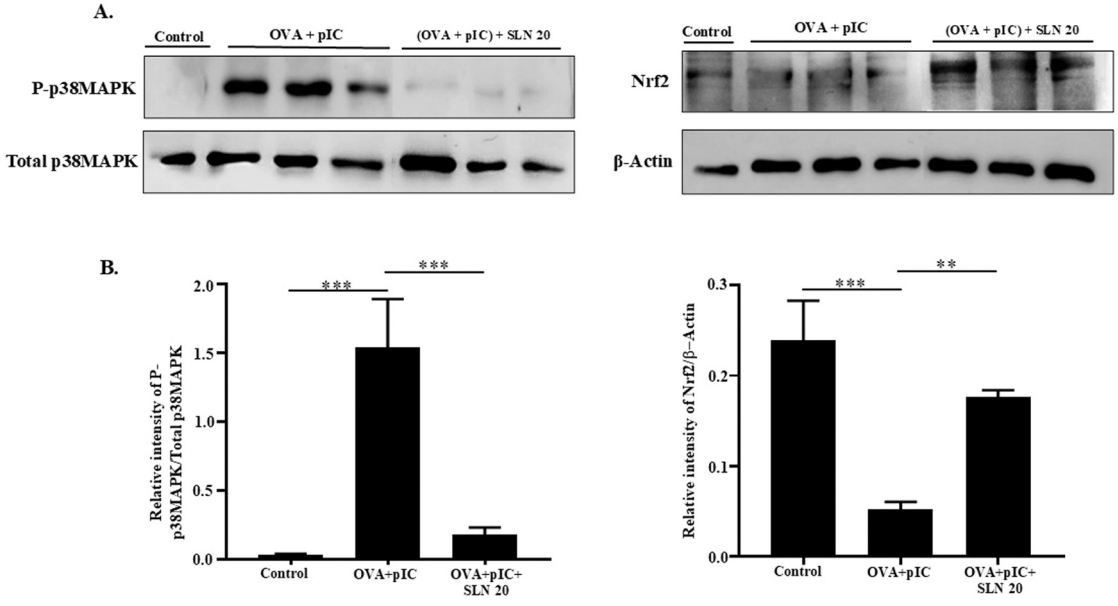


Fig. 10. Effect of curcumin-loaded SLN on protein expression of p38MAPK and Nrf2 in OVA + poly (I:C) exposed mice. (A) The phosphorylation of p38MAPK at Thr^{180}/Tyr^{182} and expression of Nrf2 in the lung tissues of different experimental groups. (B) Densitometric analysis of phospho-p38MAPK against total p38MAPK and Nrf2 against β-actin. Data is represented as mean ± SD (n = 3 animals/group). Statistical analysis was performed by one-way ANOVA followed by Tukey's multiple comparisons. **p < 0.01, ***p < 0.001. pIC: poly (I:C), SLN 20: curcumin-loaded SLN (20 mg/kg).

MAPK signalling, thereby suppressing the production of inflammatory cytokines (Rana et al., 2016). Consistent with this, we observed that treatment with curc-SLN leads to suppression of OVA + poly (I:C)-mediated p38MAPK phosphorylation in lungs of mice. Thus, it is plausible that modulation of MAPK signalling by curc-SLN represents an important mechanism to mitigate OVA + poly (I:C)-induced asthma exacerbation like phenotype.

Asthma has been well linked to the generation of reactive oxygen species (ROS), with neutrophils described as the major source of ROS (Comhair and Erzurum, 2010; Nadeem et al., 2003). To correlate the anti-inflammatory potential of curc-SLN with its anti-oxidant properties, we measured various oxidative stress parameters. OVA + poly (I:C) treatment in mice exhibit substantial increase in ROS, MDA, and protein carbonyls, accompanied by depletion of GSH. Curc-SLN restored the redox homeostasis towards normal effectively, indicating its anti-oxidant properties. The antioxidant properties of curcumin stems from its unique β-diketone structure and rich π electrons system, which confer potent free radical scavenging property through transfer of electrons or hydrogen atoms donation from phenolic sites (Barzegar and Moosavi-Movahedi, 2011). Multiple studies confirm curcumin's broad ROS-scavenging abilities; it inhibits lipid peroxidation, scavenges superoxide radicals, and interacts with stable free radicals like DPPH (Ak and Gülçin, 2008; Borra et al., 2013; Yuan et al., 2022). Moreover, curcumin has been reported to activate Nrf2, master regulator of cellular antioxidant response making it possible that curc-SLN activates Nrf2 to impede the oxidative stress generated by poly (I:C) in the lungs (Rahban et al., 2020; Ghafouri-Fard et al., 2022; Lin et al., 2019). In line with this, our data showed that curc-SLN restored the expression of Nrf2 towards normal in mice subjected to conditions mimicking virus-mediated asthma exacerbations. The ability to modulate oxidative stress markers, alongside its anti-inflammatory effects, provides a compelling mechanistic rationale for their use in managing virus-mediated asthma exacerbation. Recent reports have also demonstrated that asthma exacerbation can be aggravated by environmental stressors such as NO_2, high temperature, and high humidity, which are associated with increased inflammation, oxidative stress, AHR, and activation of transient receptor potential (TRP) channels, particularly TRPV1 (Lu et al., 2023a, 2024a, 2023b, 2024b). These findings are consistent with our observation of heightened inflammation, AHR, pathologic changes, and oxidative stress upon virus-mediated asthma exacerbation. Overall, these studies suggest that different exacerbating stimuli may converge on common downstream processes, particularly oxidative stress and inflammation, while involving distinct upstream pathways.

While the study provides important mechanistic findings, we primarily focused on acute exacerbation endpoints, long-term studies are required to determine whether curc-SLN can modify chronic airway remodelling or prevent recurrent exacerbations. Additionally, the study did not evaluate potential interactions with existing asthma management therapies particularly corticosteroids which would be essential for translational relevance in clinical settings.

Nevertheless, our findings point to the anti-inflammatory and anti-oxidant effects of curcumin-loaded SLNs as it effectively mitigates poly (I:C)-induced exacerbation of allergic asthma by suppressing neutrophilic inflammation, and restoring redox balance through inhibition of MAPK signalling, and alleviating AHR and mucus hypersecretion. These highlight curcumin-loaded SLNs as a promising preventive/therapeutic strategy for managing virus-triggered asthma exacerbations, warranting further translational investigation.

Ethics declaration

This study was conducted in accordance with the ARRIVE (Animal Research: Reporting of In Vivo Experiments) guidelines. This study was approved by the Panjab University Institutional Animal Ethics Committee. (Approval No. PU/45/99/CPCSEA/IAEC/2022/695)

Ethics approval

All animal experiments were carried in accordance with the ARRIVE guidelines, and the National Institutes of Health Guide for the Care and Use of Laboratory Animals (NIH Publications No. 8023, revised 1978). All animal experiments and protocols in the present work were performed in compliance with the "Guidelines for the Care and Use of Experimental Animals" approved by the Panjab University Institutional Animal Ethics Committee (PU/45/99/CPCSEA/IAEC/2022/695).

Compliance with ethical standards

None.

Funding

This work was supported by the DBT-BUILDER grant to Amarjit S Naura by the Department of Biotechnology, Government of India (#BT/INF/22/SP41295/2020). The grant received by Rashtriya Uchchatar Shiksha Abhiyan (RUSA), Ministry of Education, Government of India to Panjab University is highly acknowledged.

Declaration of Competing Interest

The authors have no competing interests to declare that are relevant to the content of this article.

Acknowledgement

The authors grately acknowledge Dr. Jatesh Kumar, Assistant Professor, Department of Statistics, GGDSD College, Chandigarh for his valuable expert assistance in the statistical analysis of the data.

Appendix A. Supporting information

Supplementary data associated with this article can be found in the online version at doi:10.1016/j.tice.2026.104039.

Data availability

Data will be made available on request.

References

Abd El-Hack, M.E., et al., 2021. Curcumin, the active substance of turmeric: its effects on health and ways to improve its bioavailability. J. Sci. Food Agric. 101 (14), 5747–5762.
Adcock, I.M., Ito, K., 2004. Steroid resistance in asthma: a major problem requiring novel solutions or a non-issue? Curr. Opin. Pharmacol. 4 (3), 257–262.
Ak, T.P., Gülçin, I.J.C.-bi, 2008. Antioxidant and radical scavenging properties of curcumin, 174 (1), 27–37.
Bakakos, A., et al., 2023. Epidemiology and Immunopathogenesis of Virus Associated Asthma Exacerbations. J. Asthma Allergy 16 (null), 1025–1040.
Barzegar, A., Moosavi-Movahedi, A.A.J.Po, 2011. Intracellular ROS protection efficiency and free radical-scavenging activity of curcumin. PLOS ONE 6 (10), e26012.
Bochkov, Y.A., Gern, J.E., 2016. Rhinoviruses and Their Receptors: Implications for Allergic Disease. Curr. Allergy Asthma Rep. 16 (4), 30.
Borra, S.K., et al., 2013. Antioxidant and free radical scavenging activity of curcumin determined by using different in vitro and ex vivo models. PLOS ONE 7, 2680–2690.
Bradford, M.M., 1976. A rapid and sensitive method for the quantitation of microgram quantities of protein utilizing the principle of protein-dye binding. Anal. Biochem. 72 (1), 248–254.
Burge, K., et al., 2019. Curcumin and Intestinal Inflammatory Diseases: Molecular Mechanisms of Protection. Int. J. Mol. Sci. 20, 1912. https://doi.org/10.3390/ijms20081912.
Chandel, J., Naura, A.S., 2025. PM2.5 augments cigarette smoke-induced lung inflammation in mice by driving a stronger immune response: Potential beneficial effects of oleanolic acid. Pulm. Pharmacol. & Ther. 90, 102379.
Comhair, S.A.A., Erzurum, S.C., 2010. Redox Control of Asthma: Molecular Mechanisms and Therapeutic Opportunities. Antioxid. & Redox Signal. 12 (1), 93–124.
Curren, B., et al., 2023. IL-33-induced neutrophilic inflammation and NETosis underlie rhinovirus-triggered exacerbations of asthma. Mucosal Immunol. 16 (5), 671–684.

Fan, Z., et al., 2015. Anti-inflammatory and antioxidant effects of curcumin on acute lung injury in a rodent model of intestinal ischemia reperfusion by inhibiting the pathway of NF-Kb. Int. J. Clin. Exp. Pathol. 8 (4), 3451–3459.
Feddema, J.J., Claassen, E., 2020. Prevalence of viral respiratory infections amongst asthmatics: Results of a meta-regression analysis. Respir. Med. 173, 106020.
Gera, M., et al., 2017. Nanoformulations of curcumin: an emerging paradigm for improved remedial application. Oncotarget 8 (39).
Ghafouri-Fard, S., et al., 2022. Nrf2-Related Therapeutic Effects of Curcumin in Different Disorders. Biomolecules 12 (1), 82.
Gracias, D.T., et al., 2021. Combination blockade of OX40L and CD30L inhibits allergen-driven memory TH2 cell reactivity and lung inflammation. J. Allergy Clin. Immunol. 147 (6), 2316–2329.
Grünig, G., et al., 1998. Requirement for IL-13 Independently of IL-4 in Experimental Asthma. Science 282 (5397), 2261–2263.
Ito, K., et al., 2008. Steroid-Resistant Neutrophilic Inflammation in a Mouse Model of an Acute Exacerbation of Asthma. Am. J. Respir. Cell. Mol. Biol. 39 (5), 543–550.
Kaur, M., Malik, J., Naura, A.S., 2024. Guggulsterone protects against cigarette smoke-induced COPD linked lung inflammation. Cell. Biochem. Biophys. 82 (2), 1145–1158.
Kim, C.-K., et al., 2018. Viral infections and associated factors that promote acute exacerbations of asthma. Allergy ASthma & Immunol. Res. 10 (1), 12–17.
Kolaczkowska, E., Kubes, P., 2013. Neutrophil recruitment and function in health and inflammation. Nat. Rev. Immunol. 13 (3), 159–175.
Kumari, A., Dash, D., Singh, R., 2015. Lipopolysaccharide (LPS) exposure differently affects allergic asthma exacerbations and its amelioration by intranasal curcumin in mice. Cytokine 76 (2), 334–342.
Lai, H., Rogers, D.F., 2010. New Pharmacotherapy for Airway Mucus Hypersecretion in Asthma and COPD: Targeting Intracellular Signaling Pathways. J. Aerosol Med. Pulm. Drug. Deliv. 23 (4), 219–231.
Lin, X., et al., 2019. Curcumin attenuates oxidative stress in RAW264.7 cells by increasing the activity of antioxidant enzymes and activating the Nrf2-Keap1 pathway. PLOS ONE 14 (5), e0216711.
Lu, C., et al., 2023a. Effect of NO(2) exposure on airway inflammation and oxidative stress in asthmatic mice. J. Hazard. Mater. 457, 131787.
Lu, C., et al., 2023b. Interaction of high temperature and NO(2) exposure on asthma risk: In vivo experimental evidence of inflammation and oxidative stress. Sci. Total. Environ. 869, 161760.
Lu, C., et al., 2024a. High humidity and NO(2) co-exposure exacerbates allergic asthma by increasing oxidative stress, inflammatory and TRP protein expressions in lung tissue. Environ. Pollut. 353, 124127.
Lu, C., et al., 2024b. Extreme temperatures exacerbated oxidative stress and airway inflammation in a mouse model of allergic asthma. Allergy 79 (5), 1333–1335.
Lunding, L.P., et al., 2015. Poly(inosinic-cytidylic) Acid–Triggered Exacerbation of Experimental Asthma Depends on IL-17A Produced by NK Cells. J. Immunol. 194 (12), 5615–5625.
Mei, X., et al., 2022. Poly I:C Exacerbates Airway Inflammation and Remodeling in Cigarette Smoke-Exposed Mice. Lung 200 (6), 677–686.
Nadeem, A., et al., 2003. Increased oxidative stress and altered levels of antioxidants in asthma. J. Allergy Clin. Immunol. 111 (1), 72–78.
Nakagome, K., Nagata, M., 2022. Innate Immune Responses by Respiratory Viruses, Including Rhinovirus, During Asthma Exacerbation. Front. Immunol. 13, **2022**.
Niessen, N.M., et al., 2021. Sputum TNF markers are increased in neutrophilic and severe asthma and are reduced by azithromycin treatment. Allergy 76 (7), 2090–2101.
Park, H.-W., Tantisira, K.G., 2017. Genetic Signatures of Asthma Exacerbation. Allergy Asthma Immunol. Res. 9 (3), 191–199.
Park, J.-W., et al., 2016. Copper oxide nanoparticles aggravate airway inflammation and mucus production in asthmatic mice via MAPK signaling. Nanotoxicology 10 (4), 445–452.
Peng KT, C.Y., Huang, T.Y., Chen, P.C., Chang, P.J., Lee, C.W., 2019. Curcumin nanoparticles are a promising anti-bacterial and anti-inflammatory agent for treating periprosthetic joint infections. Int. J. Nanomed. 14, 469–481.
Pérez-Figueroa, E., et al., 2021. Neutrophils: Many Ways to Die. Front. Immunol. 12, **2021**.
Puri, G., Naura, A.S., 2020. Critical role of mitochondrial oxidative stress in acid aspiration induced ALI in mice. Toxicol. Mech. Methods 30 (4), 266–274.
Rahban, M., et al., 2020. Anti-Viral Potential and Modulation of Nrf2 by Curcumin: Pharmacological Implications. Antioxidants 9 (12), 1228.
Rana, M., et al., 2016. A Standardized Chemically Modified Curcuma longa Extract Modulates IRAK-MAPK Signaling in Inflammation and Potentiates Cytotoxicity. Front. Pharmacol. 7, **2016**.
Sandhu, A., Naura, A.S., 2026. Intranasal exposure of poly (I:C) exacerbates OVA-induced allergic asthma by causing a major shift in the immune response. Toxicol. Appl. Pharmacol. 509, 117747.
Sandhu, S.K., et al., 2021. Systematic Development and Characterization of Novel, High Drug-Loaded, Photostable, Curcumin Solid Lipid Nanoparticle Hydrogel for Wound Healing. Antioxidants 10, 725. https://doi.org/10.3390/antiox10050725.
Shahid, H., et al., 2019. Immunomodulatory and Anti-Inflammatory Potential of Curcumin for the Treatment of Allergic Asthma: Effects on Expression Levels of Pro-inflammatory Cytokines and Aquaporins. Inflammation 42 (6), 2037–2047.
Sutcliffe, A., et al., 2012. Increased Nicotinamide Adenine Dinucleotide Phosphate Oxidase 4 Expression Mediates Intrinsic Airway Smooth Muscle Hypercontractility in Asthma. Am. J. Respir. Crit. Care Med. 185 (3), 267–274.
Tang, X., et al., 2021. Curcumin induces ferroptosis in non-small-cell lung cancer via activating autophagy. Thorac. Cancer 12 (8), 1219–1230.
Wadhwa, R., et al., 2019. Cellular mechanisms underlying steroid-resistant asthma. Eur. Respir. Rev. 28 (153), 190096.
Wang, W., et al., 2012. Enhanced bioavailability and efficiency of curcumin for the treatment of asthma by its formulation in solid lipid nanoparticles. Int. J. Nanomed. 3667–3677.
Wang, Y., et al., 2019. Curcumin protects the pancreas from acute pancreatitis via the mitogen-activated protein kinase signaling pathway. Mol. Med. Rep. 20 (4), 3027–3034.
Wark, P.A.B., et al., 2001. Neutrophil degranulation and cell lysis is associated with clinical severity in virus-induced asthma. Eur. Respir. J. 19 (1), 68–75.
Xu, Z., et al., 2022. Curcumin alleviates rheumatoid arthritis progression through the phosphatidylinositol 3-kinase/protein kinase B pathway: an in vitro and in vivo study. Bioengineered 13 (5), 12899–12911.
Yang, S., et al., 2022. 5-Methoxyflavone-induced AMPKα activation inhibits NF-κB and P38 MAPK signaling to attenuate influenza A virus-mediated inflammation and lung injury in vitro and in vivo. Cell. & Mol. Biol. Lett. 27 (1), 82.
Yang, X., et al., 2017. Curcumin reduces lung inflammation via Wnt/β-catenin signaling in mouse model of asthma. J. Asthma 54 (4), 335–340.
Yong, H.-Y., Koh, M.-S., Moon, A., 2009. The p38 MAPK inhibitors for the treatment of inflammatory diseases and cancer. Expert. Opin. Investig. Drugs 18 (12), 1893–1905.
Yuan, R., et al., 2022. Fe-Curcumin Nanozyme-Mediated Reactive Oxygen Species Scavenging and Anti-Inflammation for Acute Lung Injury. ACS Cent. Sci. 8 (1), 10–21.